

# A CFD Study of Twin Impinging Jets in a Cross-Flow

Daniel Ostheimer<sup>1</sup> and Zhiyin Yang<sup>\*,2</sup>

<sup>1</sup>Department of Aeronautical and Automotive Engineering, Loughborough University Loughborough LE11 3TU, UK

<sup>2</sup>Department of Engineering and Design, The University of Sussex, Brighton BN1 9RH, UK

**Abstract:** A very complicated three-dimensional (3D) flow field is generated beneath a Vertical/Short Take-Off and Landing (VSTOL) aircraft when it is operated near the ground. This flow field can be represented by the configuration of twin impinging jets along the spanwise direction in a cross-flow. This paper describes a Computational Fluid Dynamics (CFD) study of this flow using the Reynolds Averaged Navier-Stokes (RANS) approach with a Reynolds Stress Model (RSM). The use of an RSM potentially offers a compromise between the computational efficiency of a two equation turbulence model and accuracy closer to that of Large Eddy Simulation (LES) although it will not be as accurate as LES. The current numerical results are validated against experimental data and the mean velocity profiles are reasonably well predicted by both the standard k- $\epsilon$  model and the RSM with slightly better prediction by the RSM. However, the Reynolds stress prediction by the RSM is poor compared with the experimental data, indicating that to capture the detailed unsteady flow features an LES is needed.

**Keywords:** CFD, RANS, LES, RSM, VSTOL, Twin impinging jets, Cross-flow.

## 1. INTRODUCTION

Studying twin impinging jets along the spanwise direction in a cross-flow is directly relevant to the understanding of a very complex 3D flow field generated underneath a vertical/short take-off and landing (VSTOL) aircraft operating close to the ground. It has been long recognized that, when an aircraft is in this condition, there are a great number of complexities associated with the three dimensional flow field created underneath the aircraft. The main area of concern is the possibility of ingestion of hot gases from the jet exhausts back into the engine, known as Hot Gas Ingestion (HGI). The HGI comes from the interaction of the impinging jet on a ground plane being re-circulated either in an up-wash fountain *via* encroachment along the aircraft to the intakes in the near field, or in the far field when there is a head wind. The head wind causes the flow along the ground to deflect upwards creating a vortex back towards the intakes. This will increase the intake air temperature and less content of oxygen, potentially leading to compressor stall and causing a dramatic engine thrust loss [1, 2].

Research into the effects created by a VSTOL aircraft started in the 1960s due to the technological advances that were realized with lightweight gas turbine engines and several experimental studies have been carried out by Cox and Abbot [3], McLemore *et al.*, [4] and Kuhn [5]. Cox and Abbot [3] performed several tests including simulating a headwind so that its effects could be examined. They found

that the turn-back point occurs slightly later with a stationary jet than with a moving jet, presumably because the relative motion of the ground contributed to the retardation of the wall jet flow. They performed tests on vertical and inclined jets and studied the transient effects of their deflection. McLemore *et al.*, [4] carried out wind tunnel experiments on a VTOL aircraft. Their investigation concentrated on HGI and included tests of several exhaust-nozzle configurations at a range of heights and was conducted over a range of forward speeds. The HGI into the inlets was found to be dependent upon the aircraft configuration and wind speed. The configuration with the least amount of HGI was an 'in-line' twin nozzle, which is similar configuration to the new STOVL aircraft, the Joint Strike Fighter/F-35 by Lockheed. Kuhn [5] found that when hovering out of ground effect the jet streams supporting the aircraft induce suction pressures on the lower surfaces producing a down load. As the hovering aircraft descends into ground effect, the jet streams impinge on the ground and form a radial wall jet flowing outward from the impingement points. He concluded that both the upwash fountain and ground vortex are involved with HGI, and the flow mechanisms are not fully understood. The fountain flow produced by multiple jets in hover is important because of the effects it has on lift and HGI so controlling it and its effects is crucial. A better understanding of the ground vortex and the hot gas cloud it creates is also needed.

An experimental study was carried out by Barata, Durao, Heitor and McGuirk [6] using a water flow rig and has been the basis for many numerical studies through the 1990's onwards. Further experimental studies have been carried out by Behrouzi and McGuirk [7, 8]. Several major conclusions can be drawn from the experimental study [6]: the upwash fountain flow is created from collision of the jets with the ground plate; intense velocity fluctuations are observed in

\*Address correspondence to this author at the Department of Engineering and Design, The University of Sussex, Brighton BN1 9RH, UK; Tel: 44 (0)1509 227231; Fax: 44 (0)1509 227275; E-mails: zhiyin.yang@sussex.ac.uk, z.yang@lboro.ac.uk, jzyang\_1999@yahoo.co.uk

the shear layers surrounding the impingement regions from the jets and the upwash fountain. The latter of which are dominated by strong curvature effects. They also performed a numerical simulation of the same flow case and concluded that calculation of the turbulent structure of the shear layers requires consideration of the individual Reynolds stresses.

Behrouzi and McGuirk [7] considered three different flow cases. Case one had no cross-flow and equal jet velocities, case two had no cross-flow and unequal jet velocities, case three had a cross-flow and equal jet velocities. Their major conclusions were that large local turbulence intensity was observed in the fountain region in case one and the opposing ground sheet flows led to a region of dominant normal stress production.

Behrouzi and McGuirk [8] furthered their experiments to include a lateral jet configuration with the inclusion of intake geometry. Three test cases were performed, with test case one having no intake geometry present, just the two impinging jets. Test case two had the intake geometry present but there was no intake flow. Test case three had intake geometry present, and there was also an intake flow present. Their study identified the effect of the re-enforcement process, occurring when the ground sheets from both jets merge together, with the penetration of the jet-plane being less than the penetration of the ground sheet for the fountain plane for all measure velocity ratios.

Experiments on this kind of very complicated flow are usually very expensive and the experimental conditions/parameters that can be tested are limited and hence computational studies have become more and more important. Many numerical studies have been performed on topics surrounding the scope of this paper but only those very relevant are briefly reviewed here. Barata, Durao, Heitor and McGuirk [6] did a numerical study as well for the same flow case of their experimental study using the RANS approach. They concluded that the numerical simulation was able to predict the gross features of the flow adequately. There was however failure to predict the turbulent structure of the fountain flow and impingement regions.

Behrouzi and McGuirk [7] also followed their experiments on the twin impinging jets with a numerical simulation, employing the  $k-\epsilon$  model with wall functions. They drew the same conclusion as was made by Barata, Durao, Heitor and McGuirk. [6], in that the gross flow features were well predicted by the  $k-\epsilon$  model.

Behrouzi and McGuirk [9] performed numerical simulations of intake ingestion using the  $k-\epsilon$  model based on the flow configuration presented in their earlier experimental work [8]. The conclusions were that the general flow features were modelled well. However, turbulent fluctuation predictions, specifically around the intake and feed pipe geometry as well as the ground vortex penetration regions were very poor, strongly indicating that further work is required to eliminate these errors, through possible application of RSM or LES to the flow case.

Chuang, Chen, Lii and Tai. [10] carried out a  $k-\epsilon$  simulation of twin jets impinging onto a flat plate with a

cross-flow. The results of the simulation were compared against the experimental results of Saripalli *et al.*, [11] and a reasonably good agreement was obtained in terms of mean flow features.

Li, Page and McGuirk [2] did two numerical studies using LES: twin impinging jets in a cross-flow and twin impinging jets through a cross-flow but including intake geometry. For the first simulation, the flow conditions were based on the experimental work performed by Barata *et al.* [6]. Overall a good agreement between the simulation and experimental results has been obtained for both the mean velocity field and turbulent quantities. Generally speaking the LES results agree much better with the experimental data than the results obtained from the  $k-\epsilon$  model. For the second simulation, an intake was added to the geometry with a mass inflow equal to that of the two impinging jets as well as feed pipes for the jets. This setup was chosen to match that used by Behrouzi and McGuirk [8] in their experimental study into HGI. The conclusions were that the dominant unsteadiness of the simulation was due to the flapping motion of the fountain, coupled with the impingement process. It was also observed that the results showed promise for LES's value for application to multiple impinging jet cases using real aircraft geometry.

An LES of a single impinging jet in cross-flow was carried out by Tang, Yang, Page and McGuirk [12] and they compared the LES results with a RANS-based  $k-\epsilon$  solution and experimental data. It was demonstrated that the LES gave much better results and clearly showed the superiority of the LES approach over the RANS approach with a  $k-\epsilon$  model. It is evident from the above review that the results obtained from the  $k-\epsilon$  model are not accurate enough while LES performs better but the computational cost of LES is still too high. This paper presents a numerical study of this flow using the RANS approach and assesses the performance of a Reynolds Stress Model (RSM) in this particular flow case. The use of an RSM potentially offers a compromise between the computational efficiency of a  $k-\epsilon$  model and the accuracy closer to that of an LES.

## 2. GOVERNING EQUATIONS AND NUMERICAL METHODS

### 2.1. RANS Governing Equations

The governing equations for any fluid flow are derived from the fundamental physical principles: conservation laws for mass, momentum and energy. These equations are fairly standard and will be briefly presented here. The current numerical study matches the experiments by Barata *et al.*, [6] with the fluid material being water so that the flow is incompressible.

The governing equations are three dimensional and time dependent and can be solved directly with very mesh to capture every details of turbulent flow. This approach is called Direct Numerical Simulation (DNS) which is, however, very demanding computationally and especially for high Reynolds number flow it is almost impossible to perform a DNS with the current computing power. For practical engineering calculations some kind of

simplification has to be taken in order to get results within a reasonable time scale and this is the so called *the Reynolds Averaged Navier-Stokes (RANS) approach*. The governing equations are time-averaged in the RANS approach and hence the obtained results are time averaged quantities. The RANS governing equations are as follows:

$$\frac{\partial \bar{U}_i}{\partial x_i} = 0 \quad (1)$$

$$\frac{\partial \bar{U}_i}{\partial t} + \frac{\partial (\bar{U}_i \bar{U}_j)}{\partial x_j} = -\frac{1}{\rho} \frac{\partial \bar{P}}{\partial x_i} + \frac{\partial}{\partial x_j} \left[ \nu \frac{\partial \bar{U}_i}{\partial x_j} \right] - \frac{\partial (\overline{u_i u_j})}{\partial x_j} \quad (2)$$

The time-averaging process introduces some unknown terms called Reynolds stresses (the last term on the right hand side of equation (2), which have to be provided by a turbulence model before the governing equations can be solved. There have been many turbulence models developed so far and this paper will investigate one of the most advanced turbulence model, called a *Reynolds Stress Model (RSM)*, which solves the Reynolds stresses using transport equations, rather than approximating them using other methods such as an eddy viscosity approach (e.g.  $k-\varepsilon$  model).

## 2.2. Reynolds Stress Model

The Reynolds stress transport equations can be derived from the Navier-Stokes equations and can be expressed as follows (neglecting body force and rotation force):

$$\begin{aligned} \frac{\partial (\overline{u_i u_j})}{\partial t} + \frac{\partial (\bar{U}_k \overline{u_i u_j})}{\partial x_k} = & - \left[ \frac{\overline{u_i u_k} \partial \bar{U}_j}{\partial x_k} + \overline{u_j u_k} \frac{\partial \bar{U}_i}{\partial x_k} \right] + \\ & \frac{\partial}{\partial x_k} \left[ \nu \frac{\partial \overline{u_i u_j}}{\partial x_k} - \overline{u_i u_j u_k} - \frac{p}{\rho} (\overline{u_i \delta_{jk}} + \overline{u_j \delta_{ik}}) \right] + \\ & \frac{p}{\rho} \left[ \frac{\partial \overline{u_i}}{\partial x_j} + \frac{\partial \overline{u_j}}{\partial x_i} \right] - 2\nu \frac{\partial \overline{u_i}}{\partial x_k} \frac{\partial \overline{u_j}}{\partial x_k} \end{aligned} \quad (3)$$

The two terms on the left hand side of the equation are the time derivative term and convection term. On the right hand side of the equation the first term represents the production by mean-flow deformation; the second term represents diffusive transport due to three contributions: molecular, turbulent and pressure diffusion; the third one is the pressure-strain term, accounting for stress redistribution due to fluctuating pressure; the fourth term is the dissipation term. Several terms in this exact transport equation need to be modelled. The turbulent diffusive transport term is modelled using a simplified version of the generalized gradient diffusion model proposed by Daly and Harlow [13] to improve stability.

$$D_{T,ij} = \frac{\partial}{\partial x_k} \left[ \frac{\mu_i}{\sigma_k} \frac{\partial (\overline{u_i u_j})}{\partial x_k} \right] \quad (4)$$

Gibson and Launder [14] proposed the following pressure-strain model using the classical decomposition approach consisting of three parts: the slow pressure-strain term, the rapid pressure strain term and the wall reflection term.

$$\phi_{ij} = \phi_{ij,1} + \phi_{ij,2} + \phi_{ij,w} \quad (5)$$

$$\phi_{ij,1} = -C_1 \rho \frac{\varepsilon}{k} \left[ \overline{u_i u_j} - \frac{2}{3} \delta_{ij} k \right]$$

$$\phi_{ij,2} = -C_2 \left[ (P_{ij} + C_{ij}) - \frac{2}{3} \delta_{ij} (P - C) \right]$$

$$\begin{aligned} \phi_{ij,w} = C_1 & \left[ \overline{u_k u_m n_k n_m} \delta_{ij} - \frac{3}{2} \overline{u_k u_i n_k n_j} - \frac{3}{2} \overline{u_k u_j n_k n_i} \right] \frac{0.4k^{1/2}}{d} \\ & + C_2 \left[ \phi_{km,2} n_k n_m \delta_{ij} - \frac{3}{2} \phi_{ik,2} n_k n_j - \frac{3}{2} \phi_{jk,2} n_k n_i \right] \frac{0.4k^{3/2}}{\varepsilon d} \end{aligned}$$

where  $C_1=1.8$ ,  $C_2=0.60$ ,  $C'_1=0.5$ ,  $C'_2=0.3$ ,  $d$  is normal distance to the wall.  $P_{ij}$  and  $C_{ij}$  are the production and the convection terms in equation (3),  $C=1/2C_{kk}$ ,  $P=1/2P_{kk}$ . The Gibson and Launder pressure-strain model is very popular and has been well tested in many cases, e.g., for a single impinging jet in a cross flow [15] and performed reasonably well, and hence is chosen here to be assessed for the current twin impinging jets case.

The modelled transport equation for the dissipation rate is:

$$\frac{\partial (\varepsilon)}{\partial t} + \frac{\partial (\varepsilon \bar{U}_i)}{\partial x_i} = \frac{\partial}{\partial x_i} \left[ \left( \nu + \frac{V_i}{\sigma_\varepsilon} \right) \frac{\partial \varepsilon}{\partial x_i} \right] + \frac{1}{2} C_{\varepsilon 1} P_{ii} \frac{\varepsilon}{\rho k} - C_{\varepsilon 2} \frac{\varepsilon^2}{k} \quad (6)$$

where  $\sigma_\varepsilon=1.0$ ,  $C_{\varepsilon 1}=1.44$ ,  $C_{\varepsilon 2}=1.92$ .

## 2.3. Numerical Methods and Computational Details

The current study has been carried out using the commercial FLUENT code which uses the finite volume method and details are widely available. A very brief description of the code, or more precisely the computational set-up will be given here. FLUENT offers a choice of two different numerical method based solvers, pressure based and density based. In the current study since the flow is incompressible so that the pressure based approach is used and the SIMPLE algorithm is employed for pressure-velocity coupling. The spatial discretization scheme used in the current study is the second order upwind method and the enhanced wall treatment (combining a two-layer model with enhanced wall functions which blends linear and logarithmic laws-of-the-wall smoothly) is employed. The standard  $k-\varepsilon$  model and a RSM as described above have been used. For both models the solution has converged after 4000 iterations with the highest residual being about 10-3 and lowest one about 10-4. The CPU time needed for the RSM is roughly 3 times of that for the  $k-\varepsilon$  model.

The computational study tries to match the experiment [6] as closely as possible. The water channel within the flow rig where the experiments took place was 1.5m long, 0.5m wide and 0.1m high. Results were obtained for a flow configuration of  $Re = 105,000$ , with twin jets set up side by side and a jet velocity ratio of 30. A laser Doppler system was used to allow measurements of flow velocity components to be recorded. This allowed for analysis of the three dimensional flow field and shear stress distribution (through fluctuating velocity components). Fig. (1) shows top view of the computational domain with the jet spacing of

$5D_j$ , channel width of  $25D_j$  and channel height of  $5D_j$ , matching the experimental geometry exactly, all based on the jet diameter  $D_j=20\text{mm}$ . The co-ordinates origin is located at the centre between the two jets on the channel top surface corresponding to the location as in the experiments with x-streamwise direction (cross flow direction), y-vertical direction (jet flow direction) and z-spanwise direction. The upstream and downstream sections were lengthened when compared to the experimental geometry to guarantee full capture of the ground vortex upstream of the jets and to ensure complete capture of the downstream behaviour of the flow.

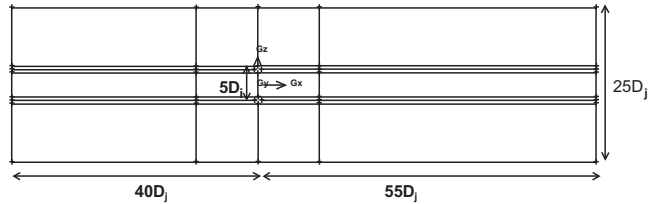


Fig. (1). Top view of the computational domain.

Since the computational domain is not complicated so that the structured mesh was chosen to achieve better numerical accuracy. Multi-block structured mesh was generated and Cartesian mesh was used in most of the computational domain while curvilinear mesh was employed to capture the round impinging jet geometry. Three separate meshes were generated and mesh sensitivity studies were carried out to make sure that the solution is mesh independent. The coarse mesh consists of 600,000 cells, the medium mesh consists of 1.2 million cells and the fine mesh consists of 2.4 million cells. Preliminary investigation demonstrated that the results obtained using the medium mesh and the fine mesh were very close so that the medium mesh was sufficient for the current study. Mesh spacing is even in the majority of computational domain with refined cells in the jet regions and near the walls, as shown in Fig. (2), to ensure that there is good mesh resolution around the impingement area of the flow, the most sensitive area within the geometry. The cell spacing in the upstream and downstream sections is slightly larger than that within the central section, as less detail is required to gather the flow features and behaviour within these regions.

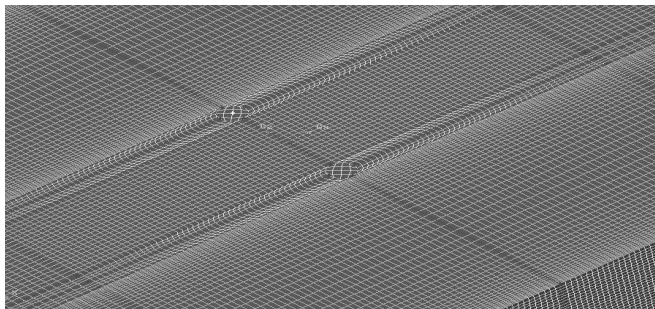


Fig. (2). Close view of mesh refinement in the jet and near wall region.

2.4. Boundary Conditions

The Reynolds number is the same as in the experiment (105,000) based on jet inlet conditions with the fluid being

water. Uniform jet and cross-flow velocities of 5.275m/s and 0.176 m/s respectively were worked out accordingly and applied at the inlet boundaries. Values of  $k$ ,  $\epsilon$  and normal stresses at jet and cross-flow inlets were derived from the measured turbulent intensities and the estimated length scales while the shear stresses were assumed to be zero. Details of the inlet boundary conditions are given in Table 1. A zero gradient boundary was applied at the outlet. No slip wall boundary condition was applied at all other boundaries.

Table 1. Details of Inlet Boundary Conditions

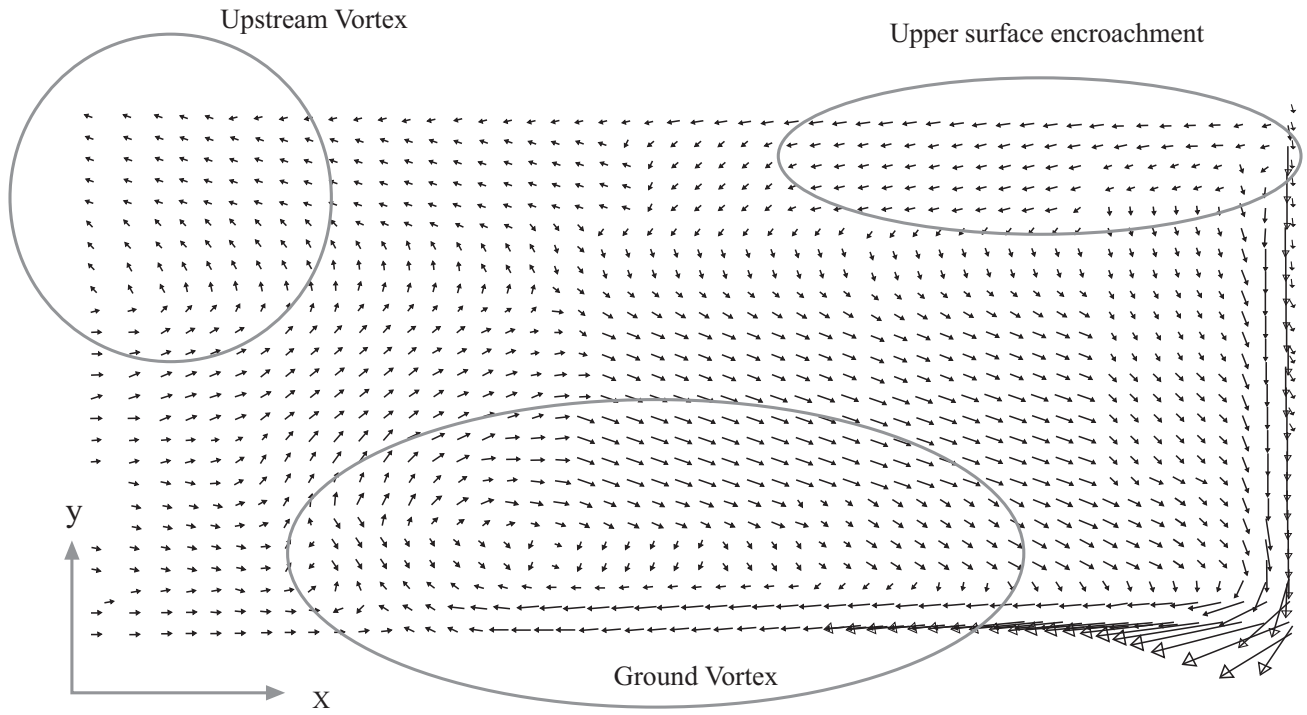
Variables	Values
Cross flow inlet velocity	0.175842 m/s
Jet flow inlet velocity	5.275245 m/s
Cross flow inlet turbulent kinetic energy	$9.0856 \times 10^{-7} \text{ kg m}^2/\text{s}^2$
Jet flow inlet turbulent kinetic energy	$5.9363 \times 10^{-4} \text{ kg m}^2/\text{s}^2$
Cross flow inlet dissipate rate	$1.4193 \times 10^{-8} \text{ kg m}^2/\text{s}^3$
Jet flow inlet dissipate rate	$1.3617 \times 10^{-11} \text{ kg m}^2/\text{s}^3$
Cross flow inlet turbulent normal stresses	$6.0571 \times 10^{-7} \text{ m}^2/\text{s}^2$
Jet flow inlet turbulent normal stresses	$3.9575 \times 10^{-4} \text{ m}^2/\text{s}^2$
Turbulent shear stresses at both inlets	0

3. RESULTS AND DISCUSSION

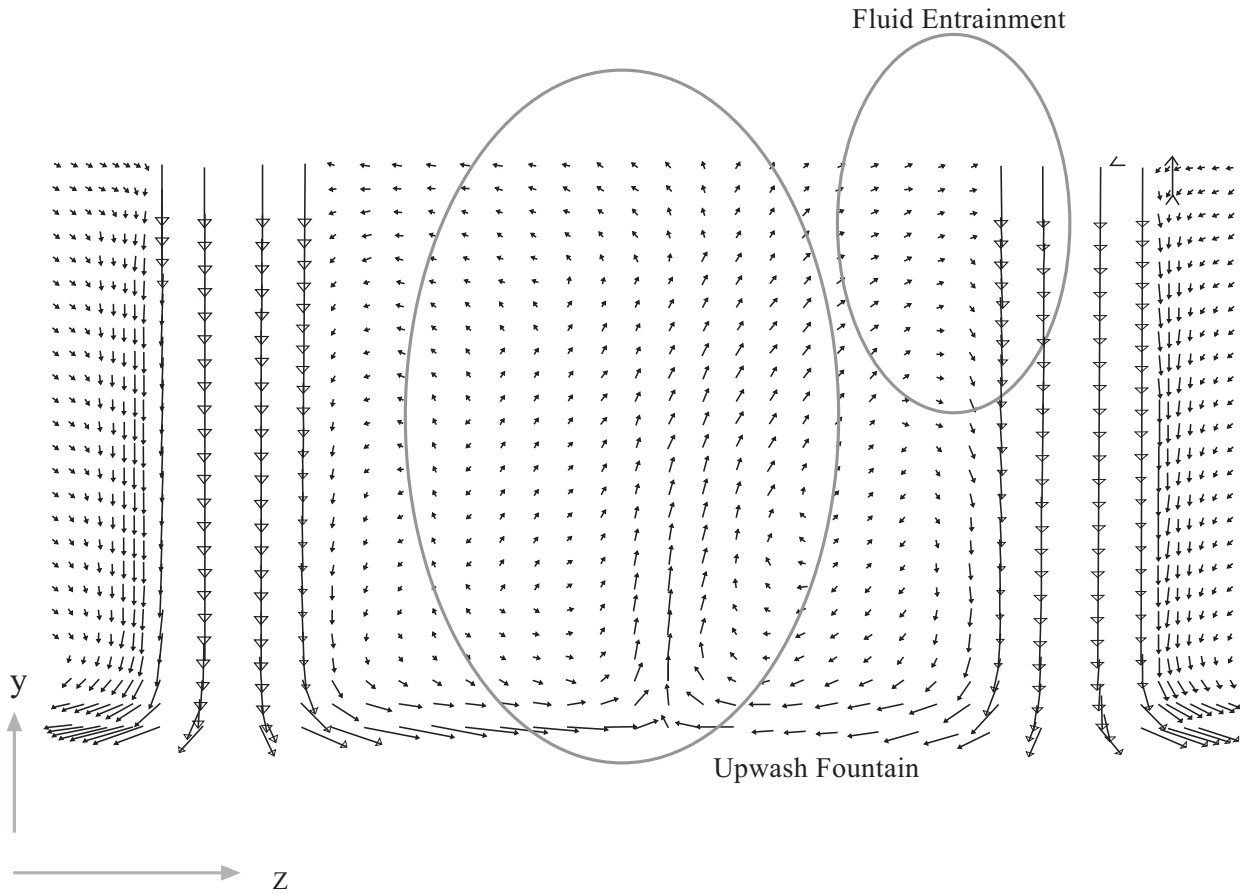
Fig. (3) shows predicted velocity vectors upstream of the jet locations in the jet plane (x, y) at  $z/D_j = 2.5$  using the RSM and three main flow features can be observed: the ground vortex resulting from the ground sheet flow from the fountain interacting with the cross-flow; fluid encroachment along the upper surface as a result of the fluid entering the flow from the jets; and a vortex upstream of the ground vortex, located near the upper surface of the channel. The RSM has predicted the location and length of the ground vortex well compared with the experimental data. The predicted ground vortex length is about  $9.2D_j$  and the measured one is about  $9.5D_j$  (the ground vortex length is defined here as the distance between tip of the ground vortex to centre of the jet, and vortex tip is defined as the point where the axial velocity is zero).

Fig. (4) shows the vector plot in the (y, z) plane across the two impinging jets at  $x/D_j = 0$ . The creation of the upwash fountain can clearly be seen here. In particular, the plot shows asymmetric behaviour of the flow in this region. The entrainment of fluid from the fountain into both jets can be seen through the vortex style flow behaviour; however this entrainment is shown to be stronger into the right jet than into the left jet.

Fig. (5) presents the comparison between the predicted mean streamwise velocity profiles along the vertical direction obtained by both the  $k-\epsilon$  model and the RSM, and the experimental data at five streamwise locations (velocity is normalized by the jet velocity, H is the channel height) in the central plane (x, y) between the jets. The predictions



**Fig. (3).** Jet plane  $(x,y)$  velocity vectors.



**Fig. (4).** Velocity vectors in the  $(y, z)$  plane showing a asymmetric fountain creation.

follow the trend of the experimental results quite well with good accuracy. The simulation appears to under-predict the influence of streamwise velocity of the ground sheet created by the impinging jets in the lower regions of the flow. Surprisingly there is very little difference between the RSM results and the  $k-\epsilon$  model results.

Fig. (6) shows the comparison between the predicted mean vertical velocity profiles obtained by both models and

the experimental data at the same streamwise locations as shown in Fig. (5). The general shape of the experimental profiles has been well captured by both models but the predicted accuracy is not as good as that of the mean streamwise velocity, especially at  $x/D_j = -1.5, 0$  and  $1.5$ . Unlike the mean streamwise velocity predictions it can be seen clearly that the results obtained from the RSM are closer to the experimental data. This indicates that it is more

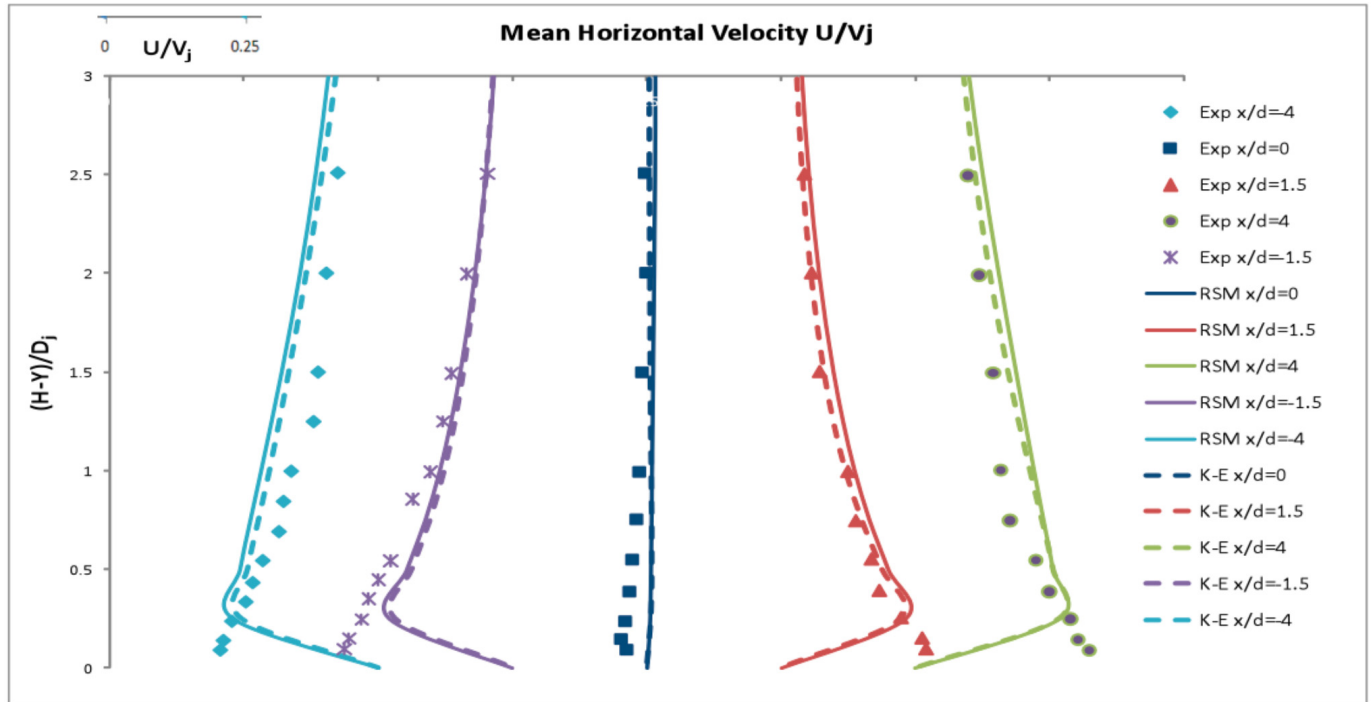


Fig. (5). Mean streamwise velocity profiles along the vertical direction at five streamwise locations.

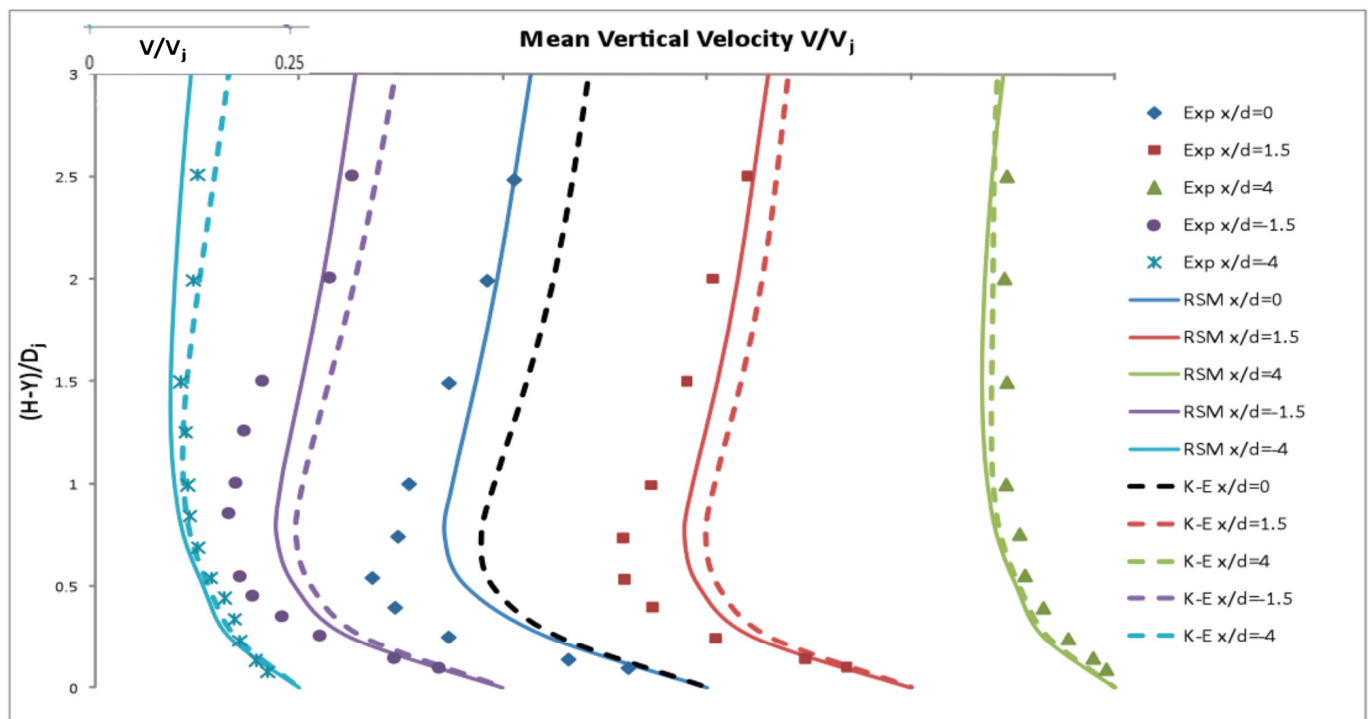


Fig. (6). Mean vertical velocity profiles along the vertical direction at five streamwise locations.

difficult to predict the mean vertical velocity accurately for this flow case.

The mean streamwise and vertical velocity profiles along the spanwise direction at three vertical locations are

presented in Figs. (7, 8). For the mean vertical velocity profiles both turbulence models perform well with good agreement between the predictions and the experimental data, and there is hardly any difference between the

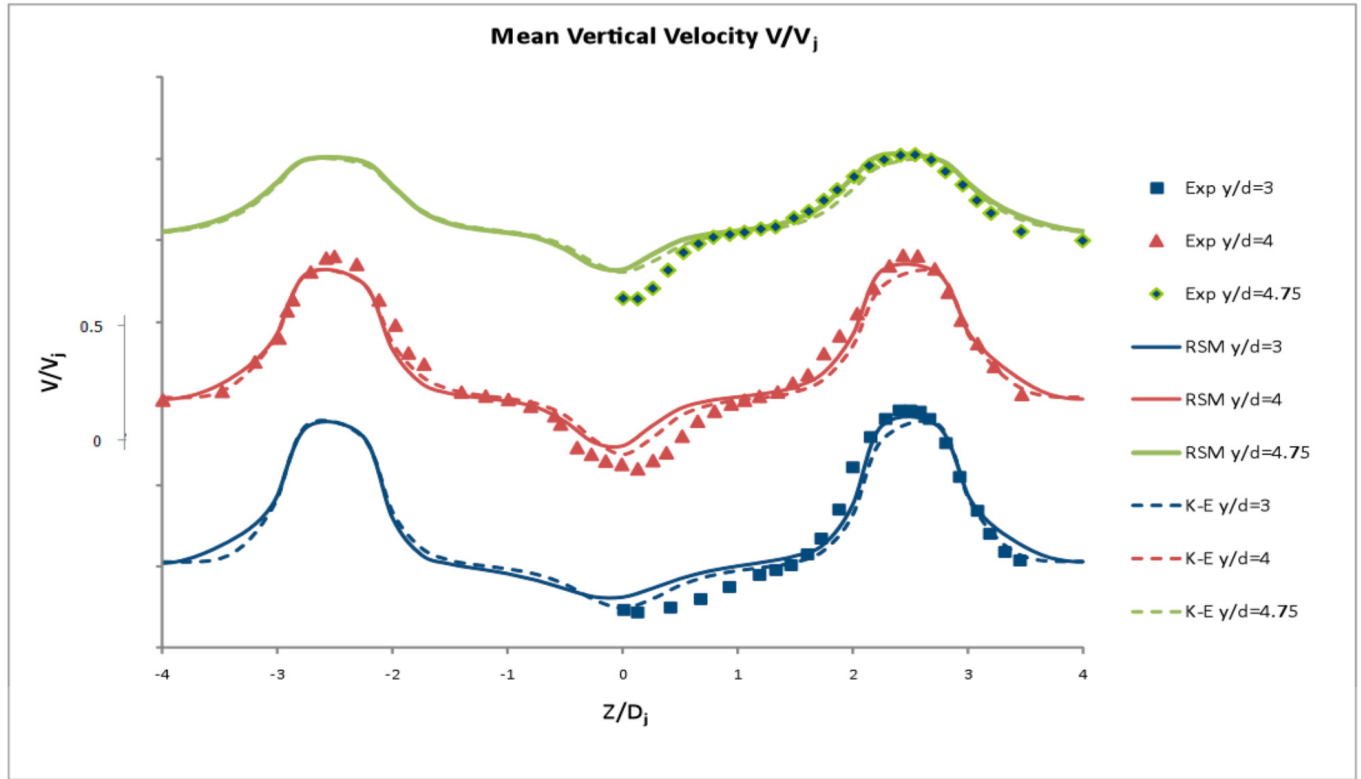


Fig. (7). Mean vertical velocity profiles along the spanwise direction at three vertical locations.

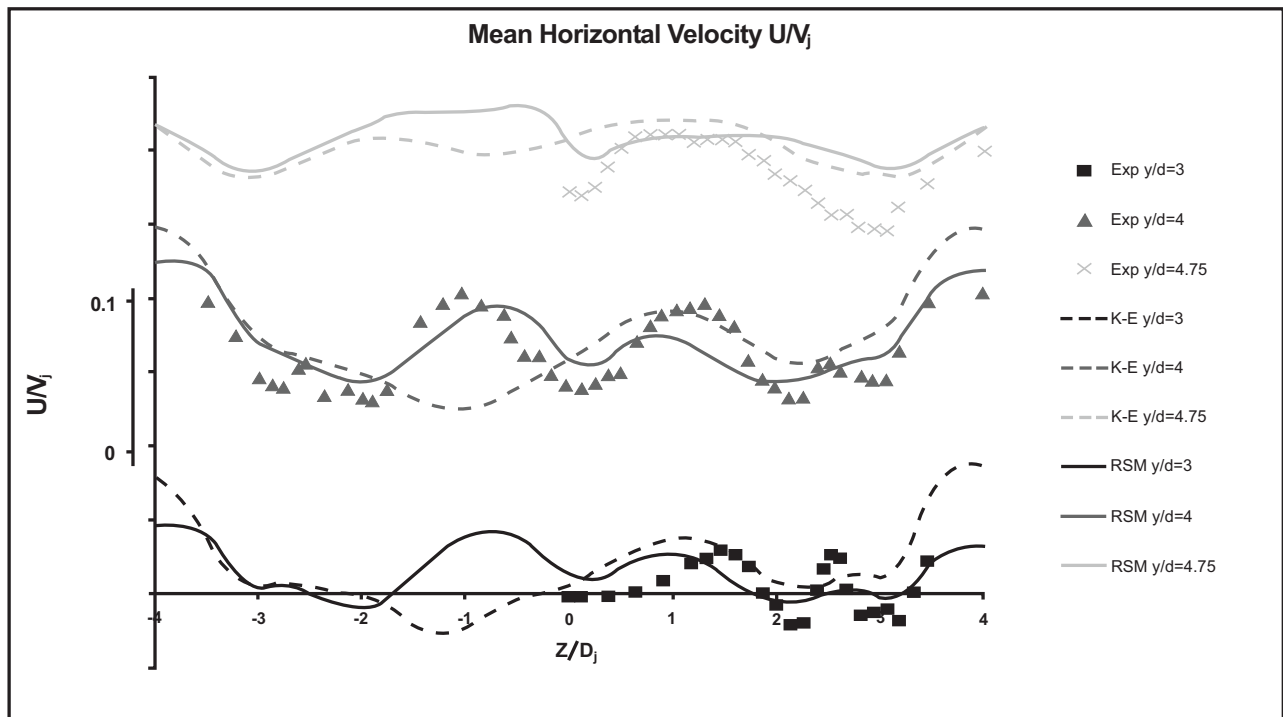


Fig. (8). Mean streamwise velocity profiles along the spanwise direction at three vertical locations.

predictions by both models. However, for the mean streamwise velocity profiles it can be seen from Fig. (8) that the RSM predictions follow the trend of the experimental results better, especially at  $y/D_j=4$  where the RSM predictions agree much better with the experimental data. Furthermore, both turbulence models predict the flow poorly at  $y/D_j=4.75$ , just below the height at which jet entry into the flow occurs. The magnitude of the influence of the jet is not captured by either set of results.

It is clear that the mean velocity field is reasonably well predicted by both models with slightly better performance from the RSM. However, it is a totally different story for the normal and shear stresses at the same locations. Fig. (9) shows the comparison between the predicted normal stress profiles in the streamwise direction and the experimental data along the vertical direction in the central plane (x, y) between the jets. It can be seen clearly from the figure that the prediction is very poor with a big discrepancy between the prediction and the experimental data. Not only the predicted stress magnitude is so much smaller but also the predicted stress profiles do not even follow the trend exhibited by the experimental results.

Similar to the normal in the streamwise direction, the normal stress in the vertical direction and the shear stress ( $u'v'$ ) are also poorly predicted at the same locations. The predicted profiles for the normal stress in the vertical direction and the shear stress follow the trend shown by the experimental slightly better compared with the normal stress in the streamwise direction but the magnitude is largely under-predicted as shown in Figs. (10, 11).

The normal and shear stress profiles along the vertical

direction in the central plane (x,y) are poorly predicted as discussed above. Nevertheless, the predicted stress profiles along the spanwise direction in the (y,z) plane provide a better agreement with the experimental data as shown in Fig. (12). The predicted normal stress in the streamwise direction show all the key features identified by the experimental data at  $Z/D_j = 2$  and 3.5, locations immediately either side of the jet.

The influence of the jet is also present close to the ground at  $Y/D_j = 4.75$  but the predictions do not quite capture this. For all three profile locations, the general trend is well followed towards the outer sides of the flow and around the jet location, however within the fountain region the predictions do not closely follow the trends identified by the experimental results. Similar predictions have been obtained for the normal stress in the vertical direction as shown in Fig. (13).

The poor predictions of turbulent stresses are mainly due to the fact that the flow field is very complicated and dominated by several very unsteady flow features (ground vortex, possible flapping of fountain vortices etc.) which the RANS approach with any turbulence models could not capture these unsteady flow features accurately at all.

**CONCLUSIONS**

This paper has presented a CFD study of twin impinging jets through a cross-flow using the RANS approach with a Reynolds stress model and the standard *k-ε model*. The flow considered is representative of the complex flow field underneath a vertical/short take-off and landing aircraft operating very close to the ground. A better understanding of

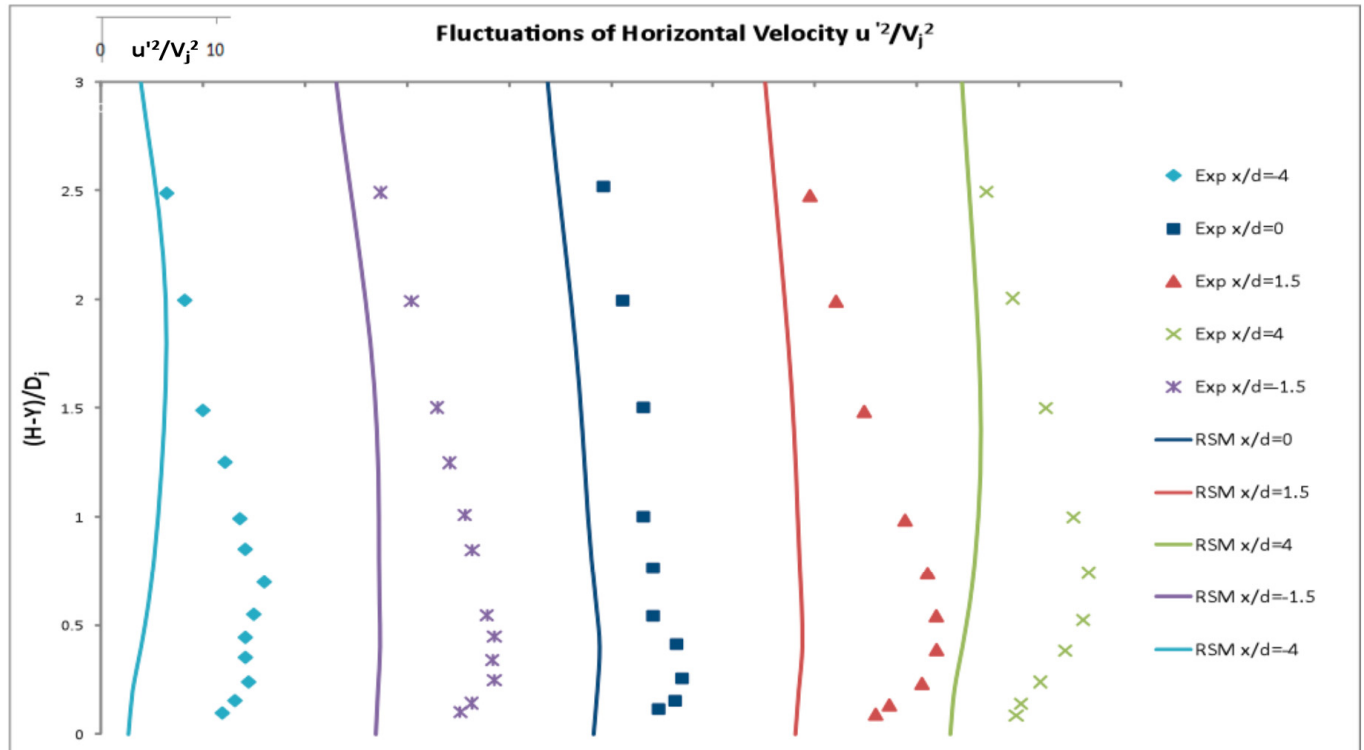


Fig. (9). Comparison between the predicted normal stress in the streamwise direction and the experimental data.

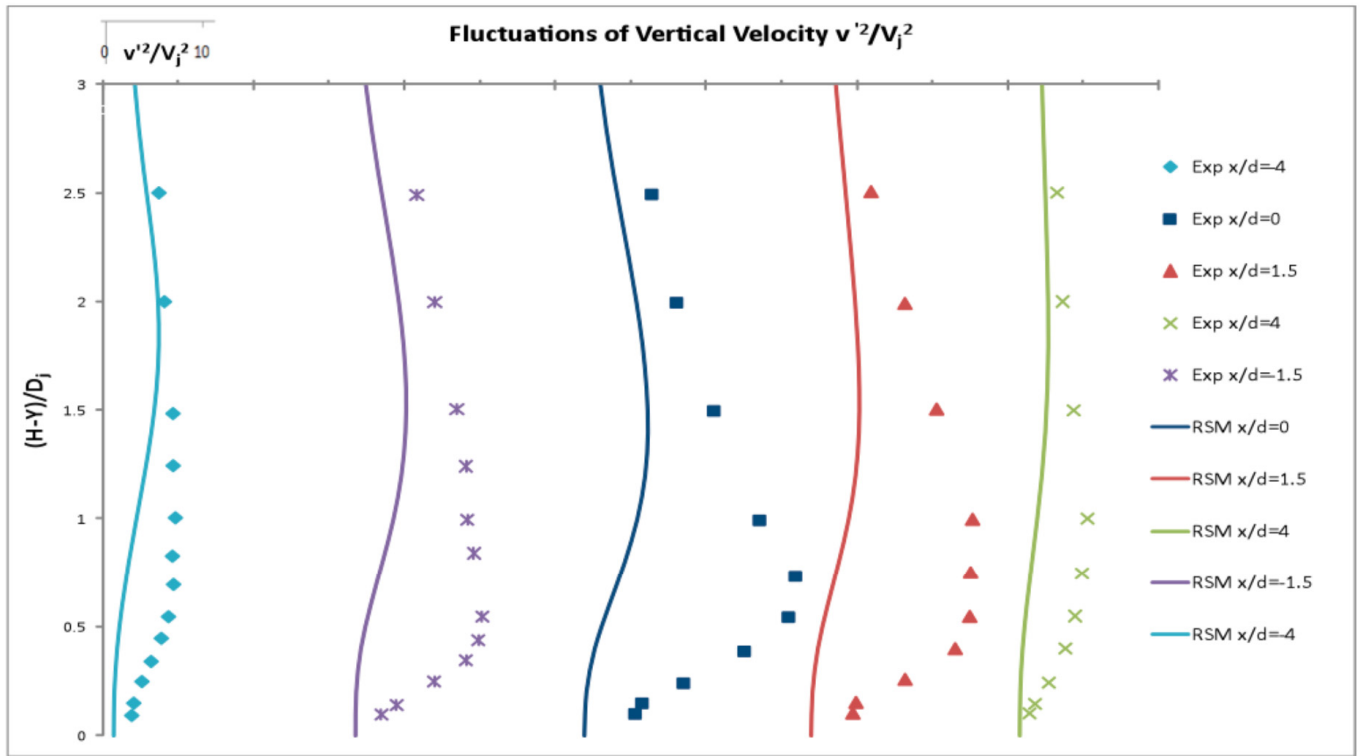


Fig. (10). Comparison between the predicted normal stress in the vertical direction and the experimental data.

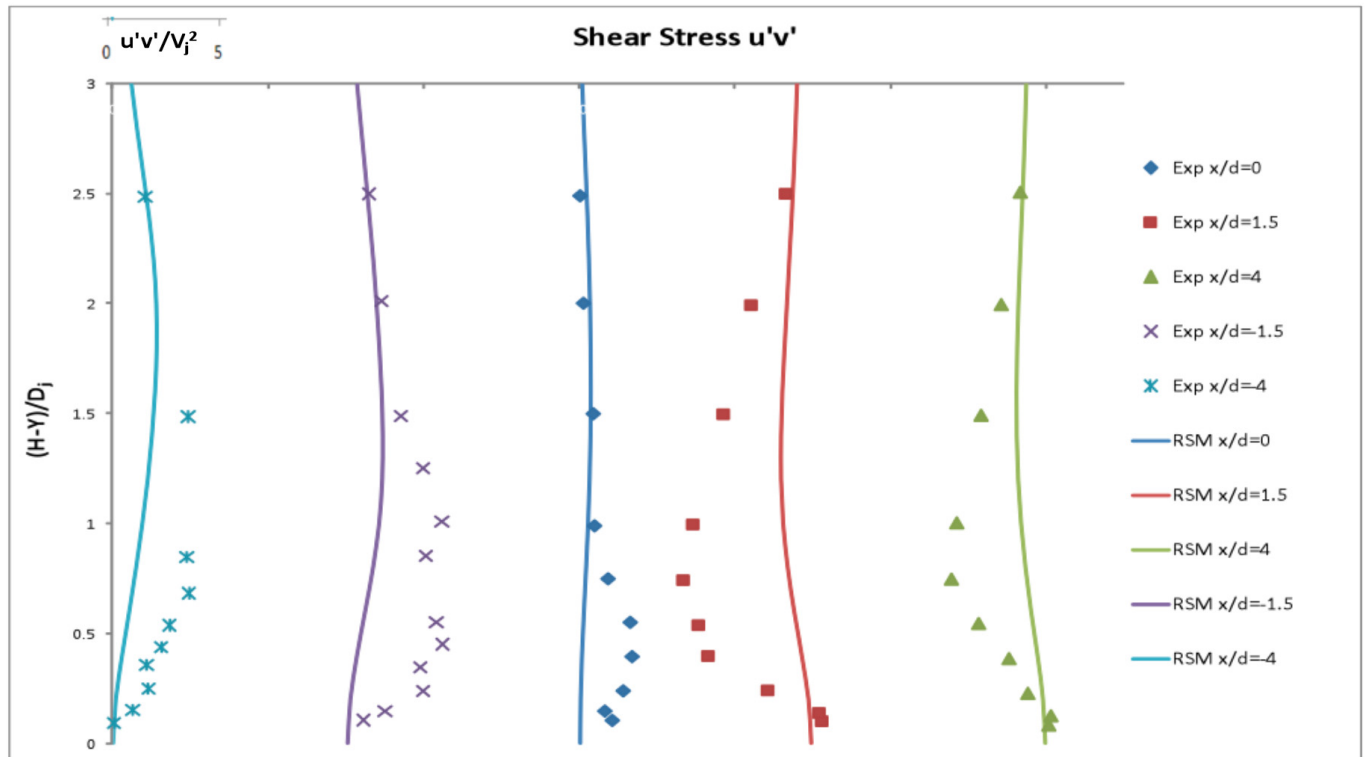


Fig. (11). Comparison between the predicted shear stress and the experimental data.

the flow field has been achieved as well as identifying the strengths and weaknesses of the RSM for this particular arrangement.

Both the *k-ε model* and the *RSM* performed well overall as far as the mean flow field is concerned, showing good

trend of the experimental results as well as good accuracy. Comparing with the experimental data the RSM prediction for the mean velocity profiles is only slightly better than that of the *k-ε model*. There were, however, a number of regions and properties of the flow, i.e., Reynolds stress, that the

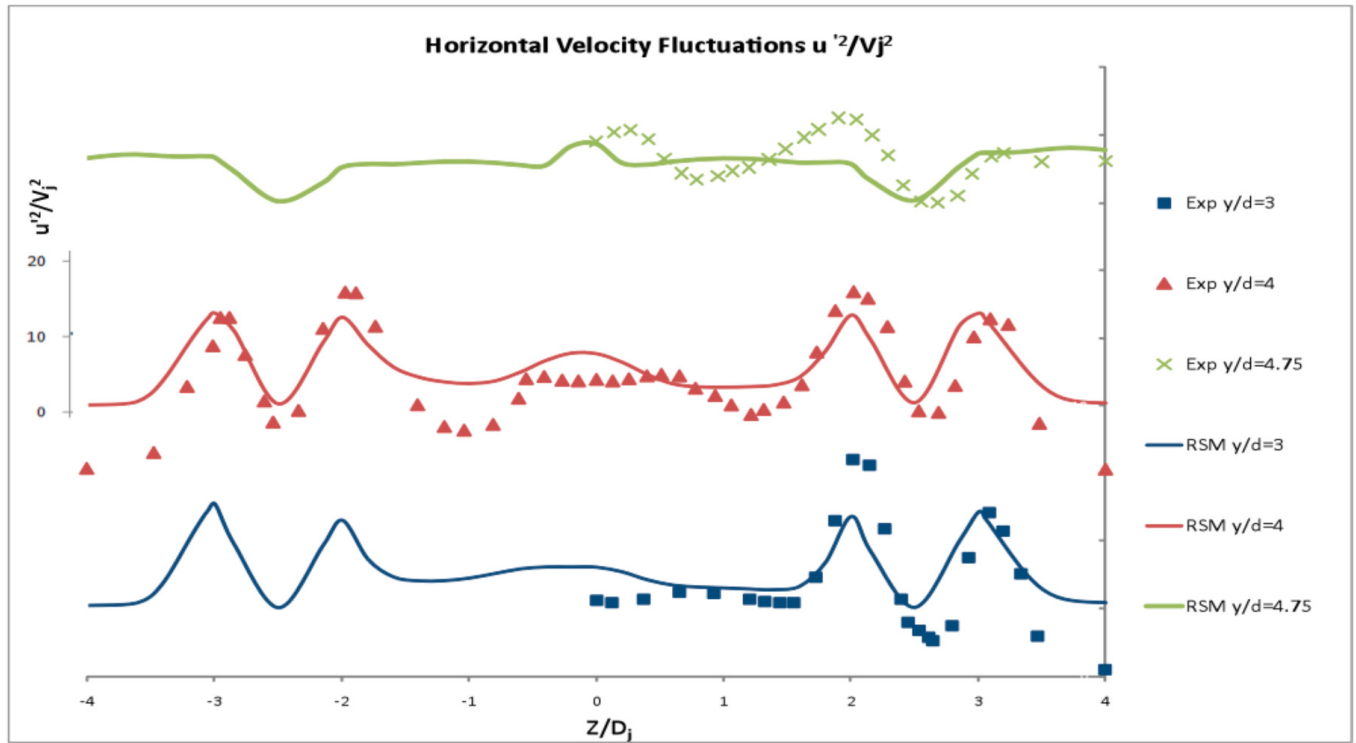


Fig. (12). Comparison between the predicted normal stress in the streamwise direction and the experimental data.

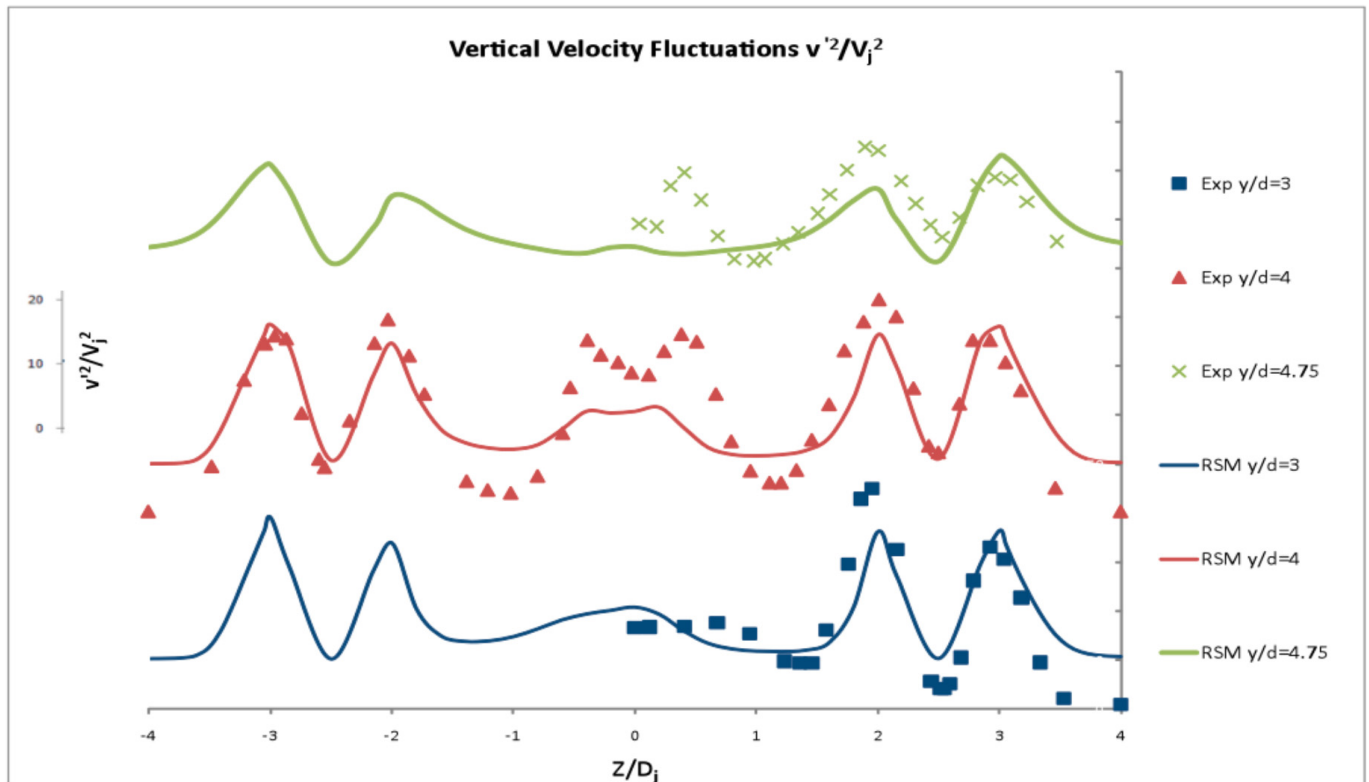


Fig. (13). Comparison between the predicted normal stress in the vertical direction and the experimental data.

RSM struggled to accurately predict. An important region of the flow that the RSM simulation struggled to predict accurately was that of the upwash fountain created between the two impinging jets. In particular, along the vertical direction in the centre plane between the jets, performance of

the RSM to predict turbulent stresses was consistently bad. The predicted Reynolds stress profiles were very poor both in accuracy as well as trend compared against the experimental results while the LES results for the same case are much better as reported by Li *et al.* [2].

In overall conclusion, the flow case of twin impinging jets in a cross-flow was modeled using the RANS approach with a RSM successfully in terms of mean flow field. However, the RSM does not really show any superiority over the  $k-\epsilon$  model in this particular flow case as the mean flow field prediction is quite similar to that obtained by the  $k-\epsilon$  model. A quicker solution can be obtained employing the RANS approach than an LES. However, it is evident from the current study that the RANS approach with even a RSM is very poor in predicting turbulent quantities and hence LES is still necessary if one wants to predict more accurately the second-order turbulent quantities such as the shear and normal stresses, and to truly capture the unsteady nature of the flow.

## REFERENCES

- [1] Knowles K, Bray D. Recent research into the aerodynamics of ASTOVL aircraft in ground environment. Proc. Institute of Mechanical Engineers, Part G. J Aerosp Eng 1991; 205: 123-31.
- [2] Li Q, Page G, McGuirk JJ. Large-eddy simulation of twin impinging jets in a cross-flow. Aeronaut J 2007; 111: 195-206.
- [3] Cox M, Abbot W. Jet recirculation effects in V/STOL aircraft. J Sound Vib 1966; 3: 393-406.
- [4] McLemore H, Smith C, Hemeter P. Generalized hot-gas ingestion investigation of large-scale jet VTOL fighter-type models. NASA TN D-5581, 1970.
- [5] Kuhn R. V/STOL and STOL ground effects and testing techniques. NASA N87-24411, 1987.
- [6] Barata J, Durao D, Heitor M, McGuirk JJ. Impingement of single and twin turbulent jets through a cross-flow. AIAA Stud J 1991; 29: 595-602.
- [7] Behrouzi P, McGuirk JJ. Laser doppler velocimetry measurements of twin-jet impingement flow for validation of computational models. Opt Lasers Eng 1998; 30: 265-77.
- [8] Behrouzi P, McGuirk JJ. Experimental data for CFD validation of the intake ingestion process in STOVL aircraft. Flow Turbulence Combustion 2000; 64: 233-51.
- [9] Behrouzi P, McGuirk JJ. Computational fluid dynamics prediction of intake ingestion relevant to short take-off and vertical landing aircraft. Proc. Institute of Mechanical Engineers, Part G. J Aerosp Eng 1999; 213: 131-42.
- [10] Chuang S, Chen M, Lii S, Tai F. Numerical simulation of twin-jet impingement on a flat plate coupled with cross-flow. Int J Numer Methods Fluids 1992; 14: 459-75.
- [11] Saripalli, K, Kroutil J, Van Horn J. Experimental investigation of hover flowfields in water at the McDonnell Douglas Research Laboratories. AGARD-CP-413, 1986.
- [12] Tang G, Yang Z, Page G, McGuirk JJ. Simulation of an impinging jet in crossflow using an LES method. Biennial International Powered Lift Conference and Exhibit, AIAA 2002-5959, 2002.
- [13] Daly BJ, Harlow FH. Transport equations in turbulence. Phys Fluids 1970; 13: 2634-49.
- [14] Gibson MM, Launder BE. Ground effects on pressure fluctuations in the atmospheric boundary layer. J Fluid Mechanics 1978; 86: 491-511.
- [15] Worth N, Yang Z. Simulation of an Impinging Jet in a Crossflow using a Reynolds Stress Transport Model. Int J Numer Methods Fluids 2006; 52: 199-211.

Received: October 26, 2011

Revised: November 15, 2011

Accepted: November 22, 2011

© Ostheimer and Yang; Licensee *Bentham Open*.

This is an open access article licensed under the terms of the Creative Commons Attribution Non-Commercial License (<http://creativecommons.org/licenses/by-nc/3.0/>) which permits unrestricted, non-commercial use, distribution and reproduction in any medium, provided the work is properly cited.